

High Sensitivity and Wide Linearity LC-MS/MS Method for Oxylipin Quantification in Multiple Biological Samples

Xian Fu¹, Hou-Hua Yin¹, Ming-Jun Wu², Xin He¹, Qing Jiang¹, Ling-Tong Zhang¹, and Jun-Yan Liu^{1*} 

¹Center for Novel Target & Therapeutic Intervention, Institute of Life Sciences, and ²Institute of Life Sciences, Chongqing Medical University, Chongqing, P. R. China

Abstract Oxylipins are important biological regulators that have received extensive research attention. Due to the extremely low concentrations, large concentration variations, and high structural similarity of many oxylipins, the quantitative analysis of oxylipins in biological samples is always a great challenge. Here, we developed a liquid chromatography-tandem mass spectrometry-based method with high sensitivity, wide linearity, and acceptable resolution for quantitative profiling of oxylipins in multiple biological samples. A total of 104 oxylipins, some with a high risk of detection crosstalk, were well separated on a 150 mm column over 20 min. The method showed high sensitivity with lower limits of quantitation for 87 oxylipins, reaching 0.05–0.5 pg. Unexpectedly, we found that the linear range for 16, 18, and 17 oxylipins reached 10,000, 20,000, and 40,000 folds, respectively. Due to the high sensitivity, while reducing sample consumption to below half the volume of previous methods, 74, 78, and 59 low-abundance oxylipins, among which some were difficult to detect like lipoxins and resolvins, were well quantified in the tested mouse plasma, mouse liver, and human plasma samples, respectively. Additionally, we determined that analytes with multifarious concentrations of over a 1,000-fold difference could be well quantified simultaneously due to the wide linearity.  In conclusion, most likely due to the instrumental advancement, this method effectively improves the quantitative sensitivity and linear range over existing methods, which will facilitate and advance the study of the physiological and pathophysiological functions of oxylipins.

Supplementary Key words biological regulators • liquid chromatography-tandem mass spectrometry • quantitative profiling • lower limits of quantitation • reduced sample consumption • lipoxins • resolvins • plasma samples • quantitative sensitivity • linear range

Oxylipins are a group of highly bioactive metabolites, which are derived from the metabolism of PUFAs through cyclooxygenase (COX), lipoxygenase (LOX), and cytochrome P450 (CYP) branches, as well as nonenzymatic pathways (1–3). As a prominent example, prostaglandins (PGs) and thromboxanes (TXs), both

generated by oxidation of arachidonic acid (ARA) through COXs, are implicated in inflammation, allergic reaction, and cardiovascular disease (4, 5). Therefore, COXs have been developed as the targets for clinical nonsteroidal anti-inflammatory drugs (NSAIDs). Hydroxyeicosapentaenoic acids (HEPEs), the metabolites of EPA following LOX and nonenzymatic pathways, inhibit the inflammatory response in adipose tissue (6) and promote glucose uptake under cold stimulation (7). Hydroxydocosahexaenoic acids (HDHAs), produced from DHA by LOXs, inhibit endothelial cell proliferation and angiogenesis (8). LOX-mediated hydroxyoctadecadienoic acids from α -linolenic acid have considerable effects on inflammation (9). Epoxyeicosatrienoic acids (EpETrEs), the epoxide metabolites of ARA via the CYP epoxygenase pathway, can regulate blood pressure (10), alleviate acute renal injury (11), and accelerate cancer cell proliferation (12). Some HETEs generated by CYP hydrolases can constrict blood vessels (13) and regulate oxylipin metabolism during inflammation (14). CYP epoxygenase-mediated epoxyoctadecenoic acids (EpOMEs) from linoleic acid (LA) promote the migration of colorectal cancer cells (15), and their corresponding diol metabolites promote the transfer of fatty acids to skeletal muscle (16) and brown adipose tissue (17). In addition, epoxyeicosatetraenoic acids (EpETEs) generated from EPA via CYP epoxygenases alleviate contact hypersensitivity (18). Epoxydocosapentaenoic acids (EpDPAs) generated from the epoxidation of DHA via CYP epoxygenases inhibit angiogenesis (19). In brief, the pleiotropic biological functions of oxylipins draw continuous attention from the world, which urges reliable methods for quantitative analysis of oxylipins in multiple biological samples as objective scientific support.

The quantification of oxylipins is always a great challenge because some oxylipins are of extremely low concentrations in biological samples, large variations in individual samples, and high structural similarity. LC-

*For correspondence: Jun-Yan Liu, jyliu@cqmu.edu.cn.

MS/MS is most widely used to quantify oxylipins due to its high sensitivity and selectivity (20). To date, several highly sensitive methods have been developed on advanced mass spectrometers, such as Agilent 6470 (21), Sciex 6500 (22–25), and Sciex 6500 plus (26). Almost all the existing methods (27–29) provided unsatisfactory results for the low abundance oxylipins, such as lipoxins and resolvins, except for the report by Dalli *et al.* (26). However, the method developed by Dalli *et al.* was recently questioned by Dr Schebb (30), resulting in a challenge on the formation, signaling, and occurrence of specialized proresolving lipid mediators, such as lipoxins or resolvins (27). Therefore, a reliable method that could quantify these low abundance oxylipins is urgently needed to stop the above-mentioned argument. It is also of great significance to have a wide linear range for the quantitative method. The concentration of oxylipins varies largely among normal samples (25), and such variations could be amplified up to a 1,000-fold upon multiple endogenous and exogenous changes (29), which requires a method with a wide linear range to quantify the oxylipins at multifarious concentrations simultaneously by using an identical preparation protocol without additional dilution or concentration process. However, many existing methods with a linear range below three orders of magnitude require more time and complicate process in sample preparation to achieve satisfactory results for the ones with huge variations (20). Additionally, chromatographic separation is also a challenge because many isomers in the oxylipin family, such as HEPEs, HETE_s, and EpETrEs, have identical MS/MS pairs (31, 32), resulting in the separation of these oxylipins heavily rely on chromatographic behavior.

To overcome the limitations and challenges mentioned above, in this study, a new LC-MS/MS-based method was established for quantitative profiling of the oxylipin family in biological samples. The superiority of this method was validated by the application of the method to analyze the oxylipins in mouse plasma, mouse liver tissue, and human plasma samples. Compared with existing methods, the sample consumption, quantifiable analytes, and allowable concentration variations were improved extensively with acceptable separation resolution.

MATERIALS AND METHODS

Chemicals and materials

A total of 104 PUFAs, 11 deuterium-labeled internal standards, and 12-(3-cyclohexan-1-yl-ureido)-dodecanoic acid (CUDA, for calculating the recovery of internal standards and monitoring the instrumental stability) were purchased from Cayman Chemical (Ann Arbor, Michigan). Their names, abbreviations, and stock solution are detailed in [supplemental Table S1](#). Chromatographic grade methanol, ethanol, acetonitrile (ACN), ethyl acetate, chloroform, and acetic acid were purchased from Thermo Fisher Scientific (Shanghai, China).

Analytical grade glycerol was purchased from Aladdin Biochemical Technology Co., Ltd. (Shanghai, China). Ultrapure water was prepared by a Milli-Q system (Millipore, Billerica, MA). An antioxidant cocktail composed of EDTA (0.2 mg/ml), butylated hydroxytoluene (0.2 mg/ml), triphenylphosphine (1 mg/ml), and indomethacin (1 mg/ml) in ethanol/methanol/water (v/v, 1/1/2) with the chemicals were purchased from Merck (Darmstadt, Germany). Oasis PRiME HLB 3 cc (60 mg) extraction cartridges and a 20-position cartridge extraction manifold were obtained from Waters Co., Ltd. (Milford, MA). Ultrafree centrifugal filters (UFC30VV00) were obtained from Merck Millipore Ltd. (Darmstadt, Germany). A ZORBAX Eclipse Plus C₁₈ column (2.1 × 150 mm, 1.8 μm) and a corresponding guard column (2.1 × 5 mm, 1.8 μm) used for chromatographic separation were purchased from Agilent Technologies Co. Ltd. (Santa Clara, CA).

LC-MS/MS conditions

Chromatographic separation was performed on an Agilent 1290 II system (Santa Clara, CA) equipped with a ZORBAX Eclipse Plus C₁₈ column (2.1 × 150 mm, 1.8 μm). Mobile phase A (A) consisted of water with 0.1% acetic acid (v/v), and mobile phase B (B) consisted of ACN/methanol/acetic acid (860/140/1, v/v/v). Gradient condition was as follows: 0–0.25 min, 33% B; 0.25–1 min, 33%–45% B; 1–3 min, 45%–55% B; 3–8.5 min, 55%–60.8% B; 8.5–12.5 min, 60.8%–63% B; 12.5–14 min, 63%–73% B; 14–15.5 min, 73%–95% B; 15.5–17.5 min, 95% B; 17.5–17.6 min, 95%–33% B; 17.6–20 min, 33% B. A 10 μl aliquot of each sample was injected for analysis. The flow rate was 0.4 ml/min, and the column temperature was kept at 50°C. The temperature of the autosampler was approximately 20°C.

Mass spectrometry analysis was performed on a SCIEX Triple Quad™ 6500 plus QTRAP (Framingham, MA) in a negative electrospray ion mode. Curtain gas, ion source gas 1, and 2 were 40, 50, and 50 psi, respectively. Electrospray voltage was –4.5 kV and ion spray source temperature was 450°C. Analytes were detected using scheduled multiple reaction monitoring (MRM). The declustering potential, collision energy, and collision cell exit potential were optimized for the precursor ion (Q1) and product ion (Q3) of each compound by direct infusion of 100 ng/ml of standard solution at 7 μl/min. The specific Q1, Q3, and corresponding declustering potential, collision energy, and collision cell exit potential optimized for quantification are shown in [supplemental Table S2](#). MRM cycle time was 0.6 s. Except for TXB₂, TXB₂-d₄, and 2,3-dinor-6-keto PGF_{1α}, the MRM detection window for the other analytes was 60 s ([supplemental Table S2](#)). Data acquisition and processing were performed using Analyst 1.7.2 (Applied Biosystems).

Preparation of stock solution

The stock solutions of 104 oxylipins, 11 internal standards, and CUDA were prepared in methanol, with concentrations of 1, 5, and 5 μg/ml, respectively. All solutions were stored at –80°C until use.

Quantitative protocol

Quantitative analysis was performed using the internal standard calibration method. The matrix effect, lower limit of quantitation (LLOQ), linearity, accuracy, precision, and stability were evaluated by the FDA (33) and EMA (34) guidelines for bioanalytical method validation. Specifically, the matrix

effect was evaluated by internal standard normalized matrix factor at a concentration of 5 ng/ml, calculated as the ratio of the matrix factor of analyte to the matrix factor of internal standard, where the matrix factor was the ratio of the peak area in solid phase extraction (SPE) sample extract to that in blank solution (methanol). LLOQ was defined as the lowest amount on the column that could be accurately quantified, allowing for quantitative deviation and precision (expressed as relative standard deviation) of less than 20%, resulting in a peak with a signal-to-noise (S/N) ratio greater than five in line with FDA/EMA guidelines. S/N was calculated using “S/N \times 1 StdDev” in Analyst 1.7.2 software, where the noise was selected in the proximity of the target peak in the same injection. The calibrators for the linearity assay were prepared by serial dilution with methanol, and the linear range was evaluated from 0.005 to 200 ng/ml, with a constant concentration of 25 ng/ml for all deuterated internal standards. The linear calibration curve was obtained by plotting the peak area of the analyte to internal standard versus analyte concentration, where LLOQ was the lowest calibrator on the calibration curve. The deviation of calibrators should be within 15% (20% for LLOQ), and at least 75% of calibrators should meet this criterion. The linear calibration curve of each analyte was established by using a linear regression algorithm with a weighting factor of $1/x^2$ following the procedure reported by Gu *et al.* (35). Linear correlation coefficient (R) greater than 0.99 was considered acceptable. Accuracy and precision were evaluated using the recovery experiments with 100 mM PBS solution, in which sample preparation was performed using the classical SPE procedure (36) and the analytes were concentrated 5 folds. Intraday assays were performed by PBS solution spiked with concentrations of LLOQ, low quality control (LQC, 3 \times LLOQ), middle quality control (MQC, 8% of upper limit of quantification), and high quality control (HQC, 80% of upper limit of quantification), with six replicates in one day. For interday assays, the above concentrations were analyzed with 18 replicates over three consecutive days. Accuracy was assessed by the ratio of back-calculated concentration to nominal concentration, and precision was evaluated by the relative standard deviation of back-calculated concentrations. Autosampler stability (approximately 20°C) was evaluated at LQC and HQC for 24 h, and the deviation between back-calculated concentration and nominal concentration was calculated.

Real sample analysis

The superiority of the developed method was demonstrated by analyzing mouse plasma/liver and human plasma samples. Mouse plasma and liver samples were obtained from sex-matched C57BL/6 mice weighing 20–25 g (N = 10). Human plasma samples were obtained from healthy volunteers (N = 10). The collection and thereafter experiments of mouse and human samples were approved by the Ethics Committee of Chongqing Medical University. Human studies abided by the Declaration of Helsinki principles.

Plasma samples were prepared according to the SPE protocols reported previously (25), but the sample consumption was halved. Specifically, after being preconditioned with 3 ml of methanol and 3 ml of SPE solution (water/methanol/acetic acid, 950/49/1 (v/v/v)), a 60 mg Oasis PRiME HLB cartridge was preloaded with an equal volume of SPE solution as the sample, then added with 10 μ l of antioxidant cocktail (a mixture of EDTA (2 mg/ml), indomethacin (2 mg/ml), butylated hydroxytoluene (0.2 mg/ml), and triphenylphosphine (0.2 mg/ml) in water/methanol/ethanol (2/1/1, v/v/v))

and 8 μ l of internal standard solution (a mixture of 11 deuterated compounds (supplemental Table S1) in methanol, each at a concentration of 125 ng/ml), followed by loading 100 μ l of mouse plasma or 200 μ l of human plasma. After 5-min standing for mixing, the loaded mixture was run through the cartridge naturally and then washed with 3 ml of SPE solution. After vacuumed dried for 5 min, the analytes were then eluted with 1.7 ml of ethyl acetate into a clean polypropylene tube containing 5 μ l of 30% glycerol in methanol. The elute was dried in vacuum evaporation and reconstructed with 40 μ l of methanol containing 25 ng/ml of CUDA. The sample was ready for analysis by centrifugation at 14,000 *g* for 10 min at 4°C with an ultrafiltration tube. In the analysis of mouse liver tissue, 30 mg of the thawed liver was mixed with 300 μ l of CHCl₃/methanol (2/1, v/v) and 10 μ l of antioxidant cocktail. The mixture was homogenized for 80 s at 60 Hz, then into which 10 μ l of internal standard solution (125 ng/ml) was added, followed by centrifugation at 12,000 *g* for 10 min. The obtained supernatant was diluted with 2 ml of ultra-pure water, then treated with the same SPE procedure as plasma samples, and finally reconstructed with 50 μ l of methanol containing 25 ng/ml of CUDA. The injection volume for both plasma and tissue samples was 10 μ l.

RESULTS

LC-MS/MS development

Due to the high structural similarity, multiple oxylipin members had a strong response at the same MRM channels, resulting in a high risk of detection crosstalk (supplemental Table S3). HDHAs and EpDPAs were susceptible to crosstalk at ion channels such as 343.1>299.2, 343.0>281.2, 343.1>193.0, and 343.1 > 189.1. HEPEs, EpETEs, and oxo-ETEs were at a high risk of MS/MS crosstalk at 317.0>255.1, 317.1>219.0, and 317.1>167.0 ion channels. Dihydroxydocosapentaenoic acids (DiHDPAs) had a high risk of crosstalk at 361 > 153 ion channel. HETEs and EpETrEs were susceptible to MS/MS crosstalk at 319 > 275, 319 > 219.2, and 319 > 167 ion channels. Alternatively, isomers such as prostaglandin E₂ (PGE₂)/PGD₂, RvD₁/RvD₂, and 12(13)-EpOME/13-HODE also had a risk of detection crosstalk at the highest ion channel.

To avoid the MS/MS crosstalk among the above-mentioned analytes undermining their detection sensitivity and quantitative accuracy, each analyte should be quantified in a highly sensitive ion channel with satisfactory chromatographic separation from interfering isomers. Herein, the chromatographic separation was completed within 20 min by optimizing the LC program. Compared with other methods, the proposed method shortened the detection time by 1–2 min and achieved more fine separation of multiple isomers (23, 25, 36). The representative chromatograms for analytes with a high risk of detection crosstalk are shown in Fig. 1. Analytes were quantified using the highest ion channel, except for 22-HDHA and 20-HDHA that were quantified using the second highest ion channel to avoid detection interference. The separation resolution for PGE₁, PGD₁, 8(9)-EpETE,

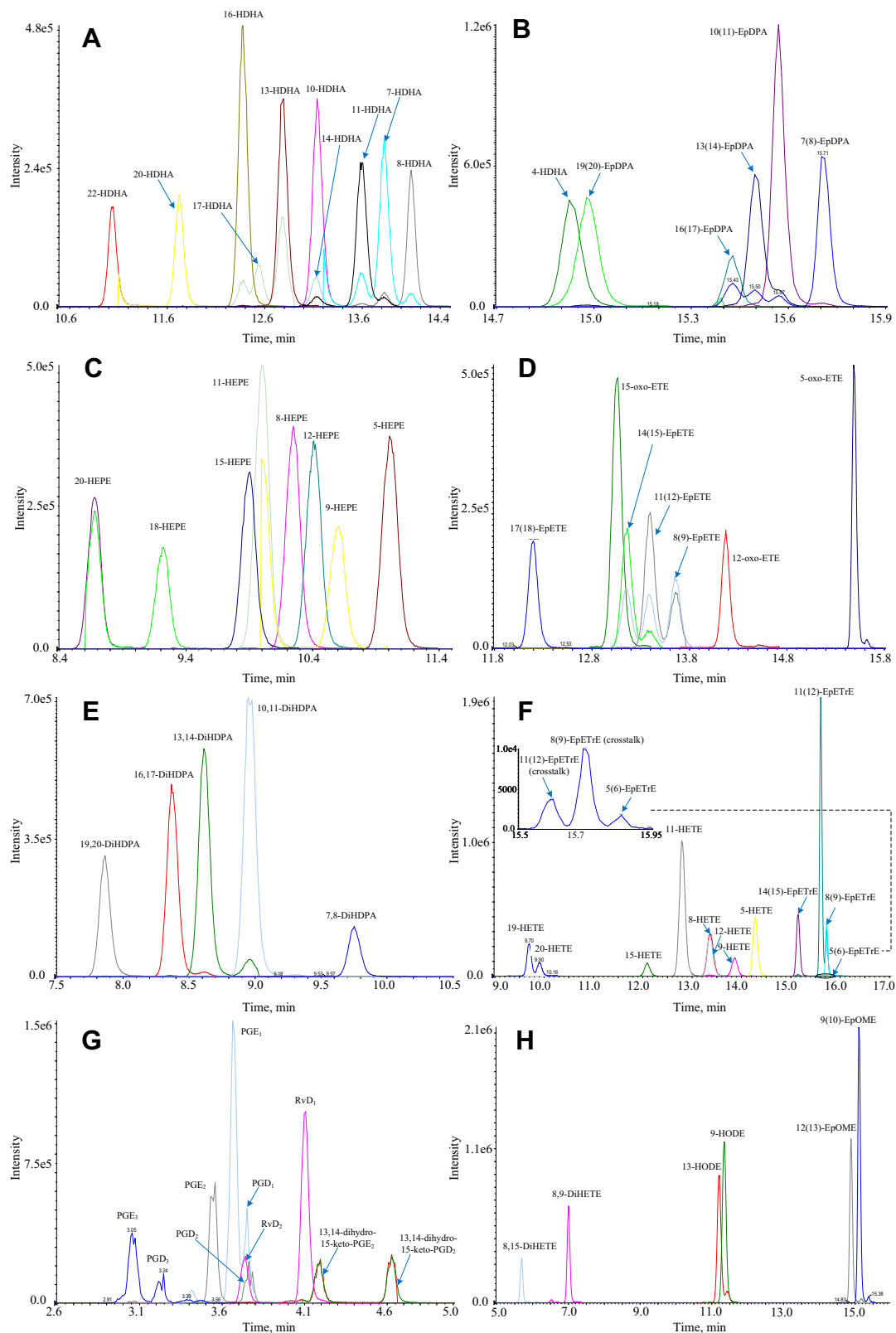


Fig. 1. Representative chromatograms for analytes with a high risk of MS/MS crosstalk. A: Ten HDHAs. B: 4-HDHA and five EpDPAs. C: Eight HEPEs. D: Four EpETEs and three oxo-ETEs. E: Five DiHDPAs. F: Eight HETEs and four EpETrEs. G: Five pairs of isomers with precursor ions at m/z 351.1, 353.3, 351.2, 349.1, and 375.2. H: Three pairs of isomers with precursor ions at m/z 335.2, 295.1, and 295.2. The risks in MS/MS crosstalk are detailed in [supplemental Table S3](#). HDHAs, hydroxydocosahexaenoic acids; EpETrEs, epoxyeicosatrienoic acids; EpDPAs, epoxydocosapentaenoic acids; EpETEs, epoxyeicosatetraenoic acids; HEPE, hydroxyeicosapentaenoic acids; DiHDPAs, dihydroxydocosapentaenoic acids; oxo-ETEs, oxo-eicosatetraenoic acids.

11(12)-EpETE, 19-HETE, 20-HETE, 17-HDHA, and 7-HDHA reached 1–1.2, and the remaining analytes achieved baseline separation ([supplemental Table S3](#)).

[Supplemental Table S2](#) summarizes the retention time (Rt) and MS/MS conditions for 104 analytes and 11 internal standards. The total ion chromatogram is shown in [supplemental Fig. S1](#). Under this condition, the detection sensitivity was extremely impressive, with 102 out of the 104 analytes with the limit of detection (LOD, $S/N \geq 3$) ranging from 0.01 to 0.5 pg and the remaining two with a LOD of 1 pg ([supplemental Table S2](#)).

Optimization of curve fitting and internal standard assignment

The quantifiable range and quantitative accuracy were related to the fitting model, the weighting factor, and the assignment of internal standards. As shown in [supplemental Table S4](#), the back-calculated accuracy for the lowest calibrator (0.005 ng/ml) with $1/x$ weighting failed to meet the criteria of 80% accuracy set by FDA and EMA, while that of $1/x^2$ satisfied it well, regardless of linear or quadratic regression and different internal standard assignments. Therefore, $1/x^2$ weighting was used in the following procedures. The optimization of the fitting model and internal standard assignment by quality control (QC) samples supported that the accuracy of linear regression was superior to that of quadratic regression, and the best quantitative results for an analyte were not necessarily obtained with its corresponding isotopic internal standard. In the case of linear regression, the quantifiable range of 5-HETE with 14,15-EpETrE- d_{11} as the internal standard spanned from 0.005 to 200 ng/ml with acceptable accuracy for all QC samples ([Fig. 2A](#)), and in contrast, the quantifiable range of 5-HETE with 5-HETE- d_8 as the internal standard was 0.005–50 ng/ml ([Fig. 2B](#)). In the case of using 5-HETE- d_8 as the internal standard for 5-HETE for quadratic regression, the accuracy of QC samples at both low and high concentrations (0.015 and 160 ng/ml) was excellent, while the accuracy was obviously lower for QC samples in the intermediate concentration range (16 and 40 ng/ml) ([Fig. 2C](#)). 14,15-DiHET confirmed a similar situation. As shown in [Fig. 2D–F](#), the optimal quantitative results for 14,15-DiHET were obtained by using 12-HETE- d_8 instead of 14,15-DiHET- d_{11} as the internal standard. The quadratic regression of 14,15-DiHET also showed that the accuracy of QC samples at low and high concentrations was excellent, while the accuracy of intermediate QC samples was unacceptable. This phenomenon for quadratic regression should be reasonable because the back-calculated accuracy for the intermediate calibrators tended to be low ([supplemental Table S4](#)).

The internal standard assignments for all analytes were optimized using linear regression with $1/x^2$ weighting to achieve superior accuracy and linear range. For this reason, 14,15-DiHET- d_{11} , 9,10-DiHOME- d_4 , and 5-HETE- d_8 were not assigned to any analyte.

[supplemental Table S5](#) shows the estimated recoveries of internal standards in the PBS by CUDA, ranging from 58.4% to 105.4%. 5(6)-EpETrE and 14,15-DiHETE failed to satisfy FDA/EMA guidelines against all internal standards. The optimal internal standards for the analytes are shown in [Table 1](#).

Matrix effect

[Supplemental Table S6](#) shows the absolute matrix factors for analytes and internal standards. Overall, the matrix effects of analytes and internal standards were acceptable, except that 12-oxo-EETE suffered from tremendous matrix enhancement of 317.9%, and 14,15-DiHETE and 11,12-DiHETE suffered from severe matrix suppression of 24.4% and 49.4%, respectively. The calibrated matrix effect for 12-oxo-EETE, 14,15-DiHETE, and 11,12-DiHETE could not meet the criterion of 85%–115% with all internal standards. Considering the matrix effect and quantitative accuracy, 12-oxo-EETE, 14,15-DiHETE, 11,12-DiHETE, and 5(6)-EpETrE could not be accurately quantified in this method. The calibrated matrix effects for the 100 analytes with the optimal internal standards ranged from 85.1% to 114.9%, complying with the criteria of 85%–115% approved by the EMA guideline ([Table 1](#)).

High sensitivity

As shown in [Fig. 3A](#), 87 oxylipins could be well quantified at 0.5 pg, and the remaining 13 oxylipins did not have such an excellent LLOQ mainly because of their inability to achieve an accuracy of 80%, even though their detection sensitivity was high ([supplemental Table S2](#)). The LLOQs of 22, 16, 25, and 24 oxylipins were validated to be 0.5, 0.2, 0.1, and 0.05 pg, respectively ([Table 1](#)). [supplemental Table S7](#) shows the LOD and LLOQ of each analyte expressed in molarity.

Wide linearity

The linear range of this method was extremely amazing. As shown in [Fig. 3B](#), there were 51 analytes with a linear range of four orders of magnitude. The less-than-excellent linear range of some analytes might be related to their property and the internal standard. The working linearity for both 9,12,13-TriHOME and 9,10,13-TriHOME was only 200-fold, similar to the previous report (36). The linear range and correlation coefficient for each compound are detailed in [Table 1](#). The linear correlation coefficients for all analytes ranged from 0.9915 to 0.9999.

Accuracy and precision

As shown in [Fig. 4](#), the accuracy for LLOQ and the other three QC samples were well within the allowable deviation of 20% and 15%, respectively, and the precision for LLOQ and the other three QC samples was well in line with the criteria of less than 20% and 15%, respectively. The results are detailed in [supplemental Table S8](#). The intra-accuracy for LLOQ, LQC, MQC,

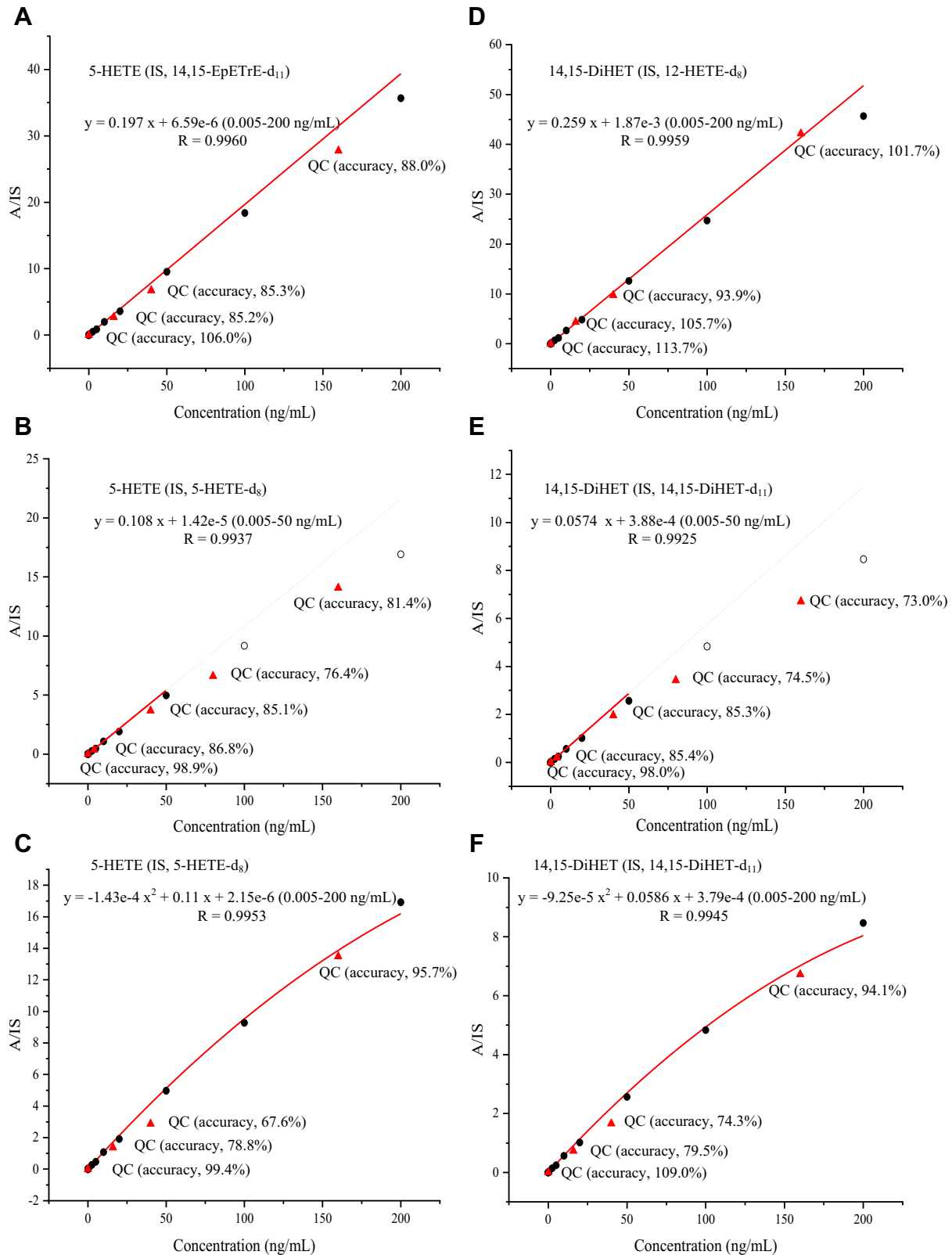


Fig. 2. Quantifiable range of 5-HETE by linear regression with $1/x^2$ weighting using (A) 14,15-EpETrE-d₁₁ and (B) 5-HETE-d₈ as the internal standard. C: Quantifiable range of 5-HETE by quadratic regression with $1/x^2$ weighting using 5-HETE-d₈ as the internal standard. Quantifiable range of 14,15-DiHET by linear regression with $1/x^2$ weighting using (D) 12-HETE-d₈ and (E) 14,15-DiHET-d₁₁ as the internal standard. F: Quantifiable range of 14,15-DiHET by quadratic regression with $1/x^2$ weighting using 14,15-DiHET-d₁₁ as the internal standard.

TABLE 1. Internal standard, calibrated matrix effect, LLOQ, linear range, and linear correlation for each analyte

Analyte	Internal Standard	Calibrated Matrix Effect (%)	LLOQ (pg)	Linear Range (ng/ml)	Linear Correlation (R)
20-OH-PGF _{2α}	9-HODE-d ₄	110.8	0.50	0.05–200	0.9961
20-OH-PGE ₂	PGE ₂ -d ₄	111.8	1.00	0.1–200	0.9962
Δ ¹⁷ -6-keto-PGF _{1α}	6-keto-PGF _{1α} -d ₄	103.2	0.50	0.05–200	0.9963
2,3-dinor-11β-PGF _{2α}	PGE ₂ -d ₄	113.1	0.20	0.02–200	0.9955
6-keto-PGF _{1α}	6-keto-PGF _{1α} -d ₄	94.0	0.05	0.005–200	0.9994
2,3-dinor-TXB ₂	TXB ₂ -d ₄	113.5	5.00	0.5–200	0.9984
RvE ₁	9-HODE-d ₄	110.9	0.20	0.02–200	0.9974
20-OH-LTB ₄	9-HODE-d ₄	104.7	0.10	0.01–200	0.9977
11-dehydro-2,3-dinor TXB ₂	14(15)-EpETrE-d ₁₁	114.7	0.50	0.05–200	0.9980
PGE ₃	PGE ₂ -d ₄	99.2	0.20	0.02–200	0.9982
2,3-dinor-6-keto PGF _{1α}	LTB ₄ -d ₄	94.6	5.00	0.5–200	0.9986
PGD ₃	PGE ₂ -d ₄	112.7	0.50	0.05–200	0.9975
9,12,13-TriHOME	LTB ₄ -d ₄	101.7	5.00	0.5–100	0.9928
PGF _{2α}	LTB ₄ -d ₄	87.0	0.50	0.05–100	0.9973
9,10,13-TriHOME	LTB ₄ -d ₄	99.3	5.00	0.5–100	0.9920
LXA ₅	14(15)-EpETrE-d ₁₁	94.4	0.10	0.01–200	0.9962
PGE ₂	PGE ₂ -d ₄	99.2	0.20	0.02–200	0.9987
TXB ₂	TXB ₂ -d ₄	93.6	0.50	0.05–200	0.9983
11-dehydro TXB ₂	14(15)-EpETrE-d ₁₁	112.3	0.10	0.01–20	0.9947
PGE ₁	LTB ₄ -d ₄	99.5	0.05	0.005–50	0.9957
RvD ₂	14(15)-EpETrE-d ₁₁	92.4	0.50	0.05–200	0.9941
PGD ₂	PGE ₂ -d ₄	99.9	0.50	0.05–200	0.9941
PGD ₁	LTB ₄ -d ₄	100.5	0.20	0.02–50	0.9974
LXA ₄	20-HETE-d ₆	114.2	0.10	0.01–200	0.9970
RvD ₁	14(15)-EpETrE-d ₁₁	109.7	0.10	0.01–200	0.9977
13,14-dihydro-15-keto PGE ₂	PGE ₂ -d ₄	114.3	1.00	0.1–200	0.9952
13,14-dihydro-15-keto PGD ₂	PGE ₂ -d ₄	86.2	0.50	0.05–200	0.9987
RvE ₂	9-HODE-d ₄	85.2	0.05	0.005–200	0.9972
PGJ ₂	LTB ₄ -d ₄	103.2	0.20	0.02–200	0.9983
LTB ₅	LTB ₄ -d ₄	94.2	0.05	0.005–20	0.9944
PGB ₂	LTB ₄ -d ₄	100.4	0.20	0.02–200	0.9969
8,15-DiHETE	12-HETE-d ₈	85.1	0.20	0.02–200	0.9960
6-trans-LTB ₄	LTB ₄ -d ₄	102.9	0.10	0.01–20	0.9941
17,18-DiHETE	12-HETE-d ₈	98.5	0.05	0.005–200	0.9939
RvD ₅	9-HODE-d ₄	98.6	0.05	0.005–200	0.9970
5,15-DiHETE	12-HETE-d ₈	90.7	0.10	0.01–200	0.9947
LTB ₄	LTB ₄ -d ₄	85.1	0.10	0.01–20	0.9953
12,13-DiHOME	9-HODE-d ₄	87.2	0.50	0.05–200	0.9966
8,9-DiHETE	12-HETE-d ₈	89.1	0.10	0.01–200	0.9951
9,10-DiHOME	9-HODE-d ₄	85.2	0.50	0.05–200	0.9958
14,15-DiHET	12-HETE-d ₈	93.5	0.05	0.005–200	0.9959
19,20-DiHDPA	14(15)-EpETrE-d ₁₁	93.2	0.05	0.005–200	0.9948
16,17-DiHDPA	14(15)-EpETrE-d ₁₁	105.4	0.05	0.005–200	0.9955
11,12-DiHET	12-HETE-d ₈	103.9	0.05	0.005–200	0.9942
13,14-DiHDPA	14(15)-EpETrE-d ₁₁	112.3	0.05	0.005–200	0.9957
20-HEPE	20-HETE-d ₆	103.1	0.20	0.02–200	0.9941
9-HOTrE	9-HODE-d ₄	89.3	0.10	0.01–200	0.9929
10,11-DiHDPA	14(15)-EpETrE-d ₁₁	107.4	0.05	0.005–200	0.9953
EKODE	14(15)-EpETrE-d ₁₁	114.2	0.50	0.05–200	0.9955
8,9-DiHET	12-HETE-d ₈	98.2	0.05	0.005–200	0.9945
13-HOTrE	9-HODE-d ₄	85.2	0.20	0.02–100	0.9957
18-HEPE	20-HETE-d ₆	97.5	0.50	0.05–200	0.9966
15-deoxy-Δ ^{12,14} -PGJ ₂	14(15)-EpETrE-d ₁₁	90.9	0.10	0.01–200	0.9973
19-HETE	20-HETE-d ₆	109.0	0.50	0.05–200	0.9969
7,8-DiHDPA	14(15)-EpETrE-d ₁₁	100.7	0.20	0.02–200	0.9969
20-HETE	20-HETE-d ₆	108.1	0.50	0.05–200	0.9980
15-HEPE	12-HETE-d ₈	102.0	0.20	0.02–200	0.9968
5,6-DiHET	12-HETE-d ₈	101.2	0.05	0.005–200	0.9953
11-HEPE	14(15)-EpETrE-d ₁₁	100.7	0.05	0.005–200	0.9942
8-HEPE	12-HETE-d ₈	95.4	0.10	0.01–200	0.9959
12-HEPE	12-HETE-d ₈	98.7	0.10	0.01–200	0.9998
9-HEPE	12-HETE-d ₈	97.9	0.10	0.01–200	0.9964
5-HEPE	14(15)-EpETrE-d ₁₁	97.4	0.10	0.01–200	0.9955
22-HDHA	14(15)-EpETrE-d ₁₁	104.9	0.10	0.01–200	0.9990
13-HODE	9-HODE-d ₄	91.4	5.00	0.5–200	0.9991
9-HODE	9-HODE-d ₄	86.3	5.00	0.5–200	0.9934
20-HDHA	14(15)-EpETrE-d ₁₁	93.7	0.20	0.02–200	0.9985
15-HETE	12-HETE-d ₈	93.6	0.10	0.01–100	0.9978
13-oxo-ODE	9-HODE-d ₄	90.8	1.00	0.1–200	0.9915
17(18)-EpETE	14(15)-EpETrE-d ₁₁	95.3	0.50	0.05–200	0.9966

(continued)

TABLE 1. Continued

Analyte	Internal Standard	Calibrated Matrix Effect (%)	LLOQ (pg)	Linear Range (ng/ml)	Linear Correlation (R)
16-HDHA	14(15)-EpETrE-d ₁₁	96.8	0.05	0.005–200	0.9968
17-HDHA	14(15)-EpETrE-d ₁₁	103.6	0.50	0.05–200	0.9962
11-HETE	12-HETE-d ₈	95.2	0.05	0.005–200	0.9955
13-HDHA	14(15)-EpETrE-d ₁₁	99.3	0.10	0.01–200	0.9966
9-oxo-ODE	9-HODE-d ₄	111.1	5.00	0.5–200	0.9935
15-oxo-EETE	14(15)-EpETrE-d ₁₁	96.9	0.10	0.01–200	0.9952
14-HDHA	14(15)-EpETrE-d ₁₁	104.9	0.20	0.02–200	0.9999
10-HDHA	14(15)-EpETrE-d ₁₁	103.3	0.10	0.01–200	0.9951
14(15)-EpETE	14(15)-EpETrE-d ₁₁	96.3	0.50	0.05–200	0.9948
8-HETE	12-HETE-d ₈	95.2	0.50	0.05–200	0.9957
12-HETE	12-HETE-d ₈	91.8	0.05	0.005–200	0.9965
11(12)-EpETE	14(15)-EpETrE-d ₁₁	100.1	0.50	0.05–200	0.9957
11-HDHA	14(15)-EpETrE-d ₁₁	99.3	0.10	0.01–200	0.9980
8(9)-EpETE	14(15)-EpETrE-d ₁₁	87.6	1.00	0.1–200	0.9973
7-HDHA	14(15)-EpETrE-d ₁₁	91.2	0.20	0.02–200	0.9952
9-HETE	12-HETE-d ₈	93.2	0.50	0.05–200	0.9969
8-HDHA	14(15)-EpETrE-d ₁₁	97.9	0.20	0.02–200	0.9948
5-HETE	14(15)-EpETrE-d ₁₁	97.6	0.05	0.005–200	0.9960
12(13)-EpOME	14(15)-EpETrE-d ₁₁	114.1	5.00	0.5–200	0.9937
4-HDHA	14(15)-EpETrE-d ₁₁	106.2	0.05	0.005–20	0.9945
19(20)-EpDPA	14(15)-EpETrE-d ₁₁	105.2	0.10	0.01–20	0.9964
9(10)-EpOME	14(15)-EpETrE-d ₁₁	114.9	5.00	0.5–200	0.9961
14(15)-EpETrE	14(15)-EpETrE-d ₁₁	94.9	0.10	0.01–200	0.9978
16(17)-EpDPA	14(15)-EpETrE-d ₁₁	104.5	0.10	0.01–20	0.9962
5-oxo-EETE	14(15)-EpETrE-d ₁₁	99.1	0.05	0.005–20	0.9952
13(14)-EpDPA	14(15)-EpETrE-d ₁₁	100.5	0.10	0.01–20	0.9942
10(11)-EpDPA	14(15)-EpETrE-d ₁₁	96.8	0.05	0.005–20	0.9953
11(12)-EpETrE	14(15)-EpETrE-d ₁₁	94.7	0.05	0.005–20	0.9967
8(9)-EpETrE	14(15)-EpETrE-d ₁₁	91.3	0.50	0.05–200	0.9944
7(8)-EpDPA	14(15)-EpETrE-d ₁₁	108.9	0.05	0.005–20	0.9943

and HQC was 82.5%–117.0%, 86.8%–115.0%, 85.5%–111.7%, and 85.2%–114.7%, respectively, and the corresponding interaccuracy was 83.3%–118.7%, 85.3%–114.8%, 85.1%–112.8%, and 85.4%–114.8%, respectively. The inter-precision for LLOQ, LQC, MQC, and HQC was 0.9%–13.4%, 1.2%–10.8%, 0.8%–12.6%, and 0.5%–11.2%, respectively, and the corresponding intra-precision was 2.4%–12.5%, 1.4%–12.2%, 1.9%–12.0%, and 1.1%–11.7%, respectively. The acceptable accuracy and precision demonstrated that our method did have the capacity to quantify over such a wide linear range.

Stability

Experiments demonstrated that the 100 oxylipins could still be accurately measured after the 24 h storage in an autosampler (about 20°C). The accuracy between the back-calculated and nominal concentrations at LQC and HQC was 87.7%–114.8% and 88.2%–114.4%, respectively (supplemental Table S9), within the acceptable deviation of 15%. It was found that 5(6)-EpETrE and 12-oxo-EETE were unstable to store in the autosampler for 24 h, with a decrease of peak area by over 25% (the note below supplemental Table S9).

Demonstration of the superiority with real samples

The superiorities of the established method were fully validated in real sample analysis. In addition to reduced sample consumption, improvements in this method were highlighted by increase in coverage of low abundance oxylipins, the number of quantifiable

oxylipins, and the ability to cover a wide range of concentration variations. supplemental Tables S10–S12 show the detailed concentrations of oxylipins in mouse plasma, mouse liver, and human plasma samples. The recoveries of internal standards in real biological samples varied in different matrices. While the internal standard recoveries in mouse and human plasma were equivalent or comparable to those in the blank matrix, those in liver tissue were less than in PBS, but acceptable (supplemental Table S5), indicating the quantitative accuracy of this method. The Rt deviations between standard solution and biological matrices are shown in supplemental Table S13. For all analytes, the Rt deviations between the standard solution and different matrices did not exceed 0.1 min. As expected, complicated biological interference increased the detection noise, as can be seen from the chromatograms of 19-HETE, 20-HETE, and 20-HEPE in different matrices (supplemental Excel S1).

High quantification capability of low abundance oxylipins

As shown in Fig. 5A, 17 and 10 analytes with mean concentrations below 0.06 ng/ml and 0.03 ng/ml were quantified in mouse plasma samples, and the mean concentration of six analytes, including PGE₃, LXA₅, PGJ₂, PGB₂, 8,15-DiHETE, and RvD₅ was even below 0.015 ng/ml (corresponding to detection concentration of 0.038 ng/ml). Similar superior sensitivity was also present in mouse tissue and human plasma samples (supplemental Fig. S2).

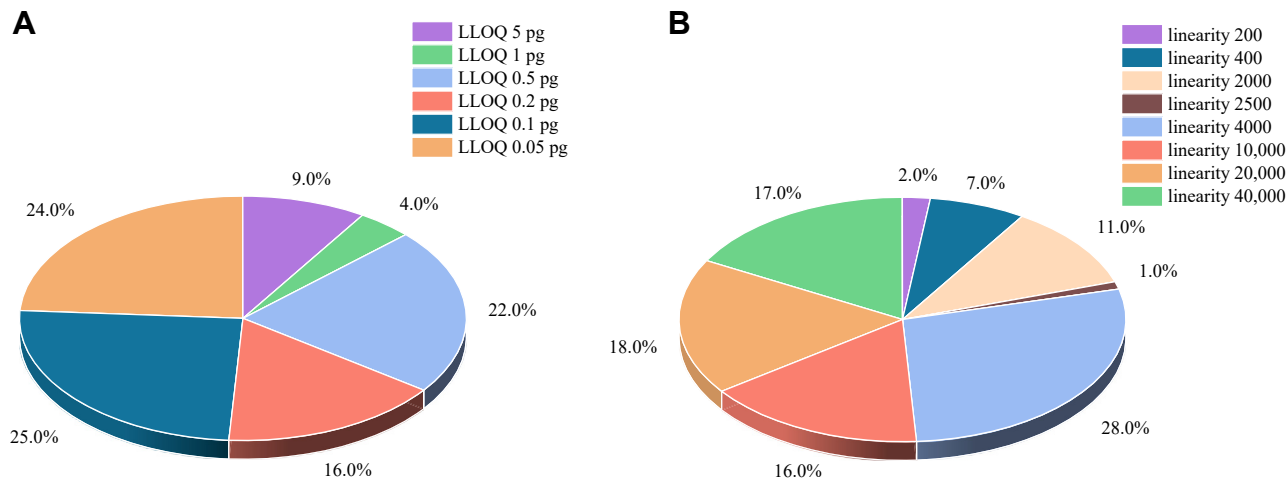


Fig. 3. Statistical plots of (A) linear range and (B) LLOQ for 100 analytes. LLOQ, lower limit of quantitation.

supplemental Excel S1 shows the chromatograms for analytes detected below 0.038 ng/ml (the chromatogram with the lowest concentration in each matrix is displayed).

The repeatability for analytes in the low-abundance samples was within 15% (supplemental Excel S1), indicating the reliability of the proposed method.

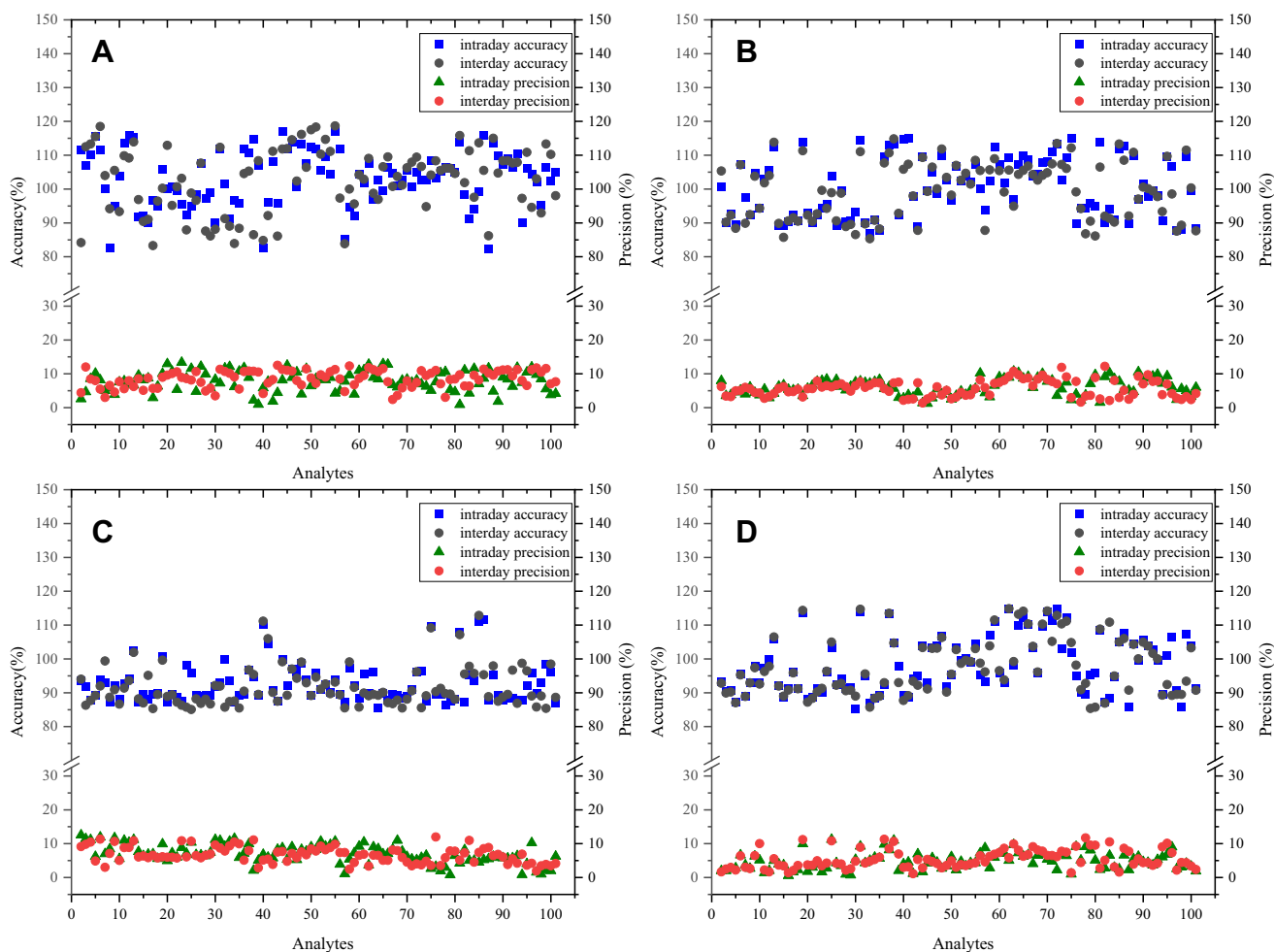


Fig. 4. The intra- and inter-accuracy and precision for (A) LLOQ, (B) LQC, (C) MQC, and (D) HQC. The details are presented in supplemental Table S8. LLOQ, lower limit of quantitation; LQC, low quality control; MQC, middle quality control; HQC, high quality control.

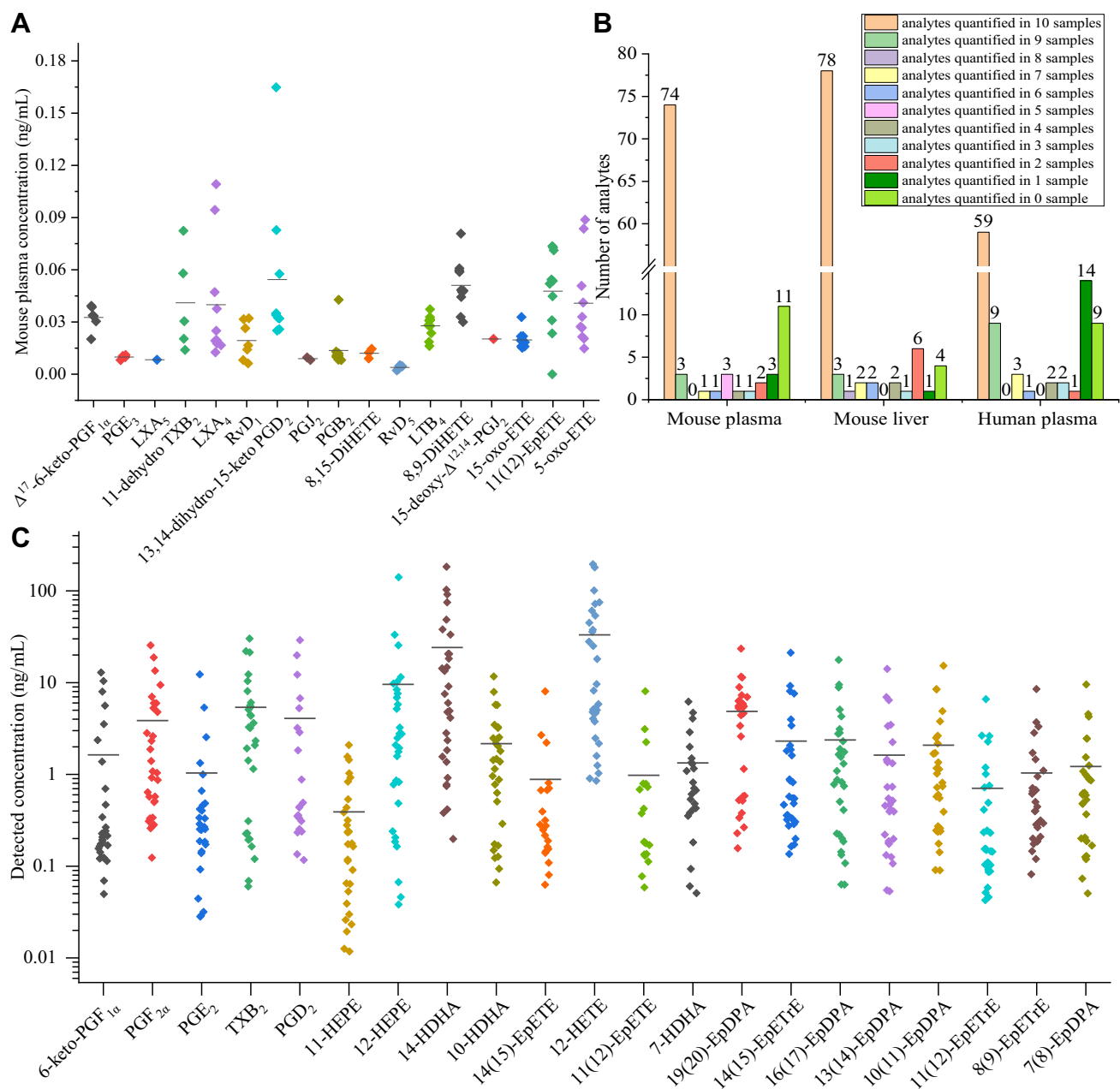


Fig. 5. A: Seventeen low-abundance analytes with an average concentration lower than 0.06 ng/ml in mouse plasma samples. B: Analytes with different detection rates in mouse plasma, mouse liver, and human plasma samples. C: Twenty one analytes with detection concentration variations of more than hundreds of times in plasma and tissue samples. The concentrations of all samples are detailed in [supplemental Tables S10–S12](#).

Competitive quantity of quantifiable oxylipins

As shown in [Fig. 5B](#), the number of analytes with 100% detection in mouse plasma, mouse liver, and human plasma samples was 74, 78, and 59, respectively, and the number of analytes with more than 67% detection in the corresponding samples was 78, 84, and 71, respectively.

High coverage of sample variations

Our method was validated to agreeably analyze both higher concentration tissue samples ([supplemental Table S11](#)) and lower concentration plasma samples

([supplemental Tables S10–S12](#)). Of all 30 samples, the quantitative concentrations of 21 analytes ranged over 100 folds, in which 12-HEPE, 14-HDHA, PGE₂, and TXB₂ ranged more than 400 folds, and 12-HEPE ranged over 3,600 folds ([Fig. 5C](#)). Simultaneous analysis of these different samples with large variations in concentration highlights the significance of a wide linear range.

DISCUSSION

In this work, the developed LC-MS/MS method has the advantages of high sensitivity and wide linearity

in quantitative profiling of oxylipins in plasma and tissue samples. In terms of sensitivity, the LLOQs for a variety of oxylipins, such as lipoxins, resolvins, PGs, HETE_s, HEPE_s, EpDPAs, and DiHDPAs are improved several fold or tens-fold ([supplemental Excel S2](#)) compared with the previous methods (21–24). Besides, the quantitative capacity for the number of oxylipins is also excellent in comparison with other reports (27–29). The improvement in the sensitivity of the present method is likely due to hardware but possibly also from the decrease in matrix effects due to the reduction in sample size as the matrix interference depends on the dilution or concentration step in the sample preparation (23). The methanol/ACN dilution method (22) was a relatively practicable way to reduce matrix interference for some analytes in comparison with the labor-intensive SPE cleanup, but the dilution method significantly decreased the concentration in the injected samples, resulting in weaker detection ability than SPE method ([supplemental Table S14](#)).

[Supplemental Table S15](#) shows the LODs of 5-HETE and 14,15-DiHET estimated by “ $3.3 \times \sigma/S$ ” (37) as the representatives, where σ was the standard deviation of the y-intercept and S was the slope of the standard curve. The results demonstrated that the LODs

estimated with “ $3.3 \times \sigma/S$ ” were close to those calculated with “ $S/N \times 1 \text{ StdDev}$ ” requiring $S/N \geq 3$ in Analyst 1.7.2 software, indicating that it was acceptable to use “ $S/N \times 1 \text{ StdDev}$ ” to calculate the S/N ratio.

Notably, lipoxins and resolvins as anti-inflammatory endogenous mediators were recently challenged by Schebb *et al.* mainly because they were unable to be monitored in most biological samples by previously reported methods (27). Surprisingly, our newly established method could quantify lipoxins (A₄ and A₅) and resolvins (E₁, E₂, D₁, and D₅) in all or part of the tested mouse/human plasma and mouse liver samples ([supplemental Tables S10–S12](#)). The chromatograms for LXA₄ and RvD₁ at the lowest concentration in each matrix are present in [Fig. 6](#). It should be noted that here, we used only the half sample volume/mass of those of other methods. It could be rationally expected that our established method could be achieved more favorable results by using the same sample volume/mass as previously reported protocols. Hence, this highly sensitive method paves a way for settling the arguments against the occurrence and functional role of these low abundance lipids. Admittedly, some analytes such as 9,12,13-TriHOME, 9,10,13-TriHOME, 13-HODE, 9-HODE, 9-oxo-ODE, 12(13)-EpOME, and 9(10)-EpOME were slightly less sensitive than that

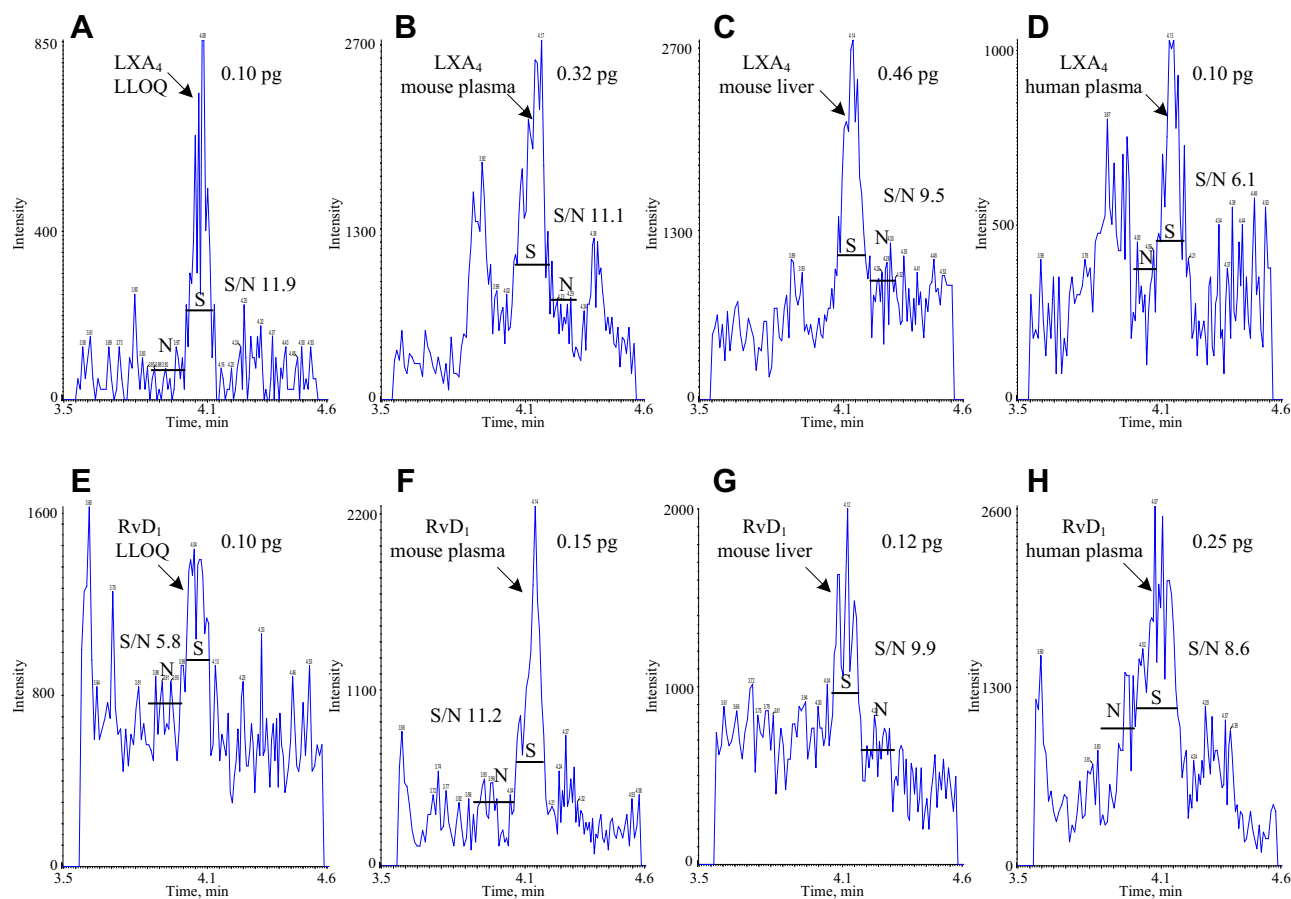


Fig. 6. Chromatograms for LXA₄ at (A) LLOQ and the lowest concentrations in (B) mouse plasma, (C) mouse liver, and (D) human plasma. Chromatograms for RvD₁ at (E) LLOQ and the lowest concentrations in (F) mouse plasma, (G) mouse liver, and (H) human plasma. Shown are the on-column amounts. LLOQ, lower limit of quantitation.

reported in the literature ([supplemental Excel S2](#)), but the proposed method could still be applied satisfactorily due to the high concentration of those analytes in biological samples. Nording *et al.* developed a sensitive assay based on Agilent 6490, but the reliability of the assay results deserves further investigation, as the concentration of LQC is hundreds to tens of thousands of times higher than their reported LLQC (38). Besides, the QTRAP 6500 plus-based assay reported by Hartling *et al.* needs to address the issue that the linear equation does not match the reported LLOQ (39).

The linearity of this method is superb. As mentioned above, a wide linear range is critical because the oxylipin levels can vary thousands of folds across individuals or experimental conditions (29). There were over 50 oxylipins with linear ranges spanning four orders of magnitude, allowing simultaneous detection of both low and high concentrations without additional dilution or concentration. In our validation samples, the analytes with the variation of 3,600 folds were well qualified by this method without any additional dilution. For most analytes, the linear range of this method is several to tens of times better than that reported in the literature ([supplemental Excel S2](#)). The improvement in the linear range is mainly attributable to the advances in instrumentation. It is undeniable that in addition to oxylipins, linear ranges spanning tens of thousands are also rarely reported for quantitative analysis of other analytes.

Good chromatographic separation is a prerequisite for accurate quantification. Our method simultaneously separated multiple structurally similar oxylipins such as HDHAs, EpDPAs, HEPEs, and EpETEs, which is rarely reported in other studies (27–29). We failed to achieve a rapid separation of multiple isomers within 5 min for acceptable accuracy according to the method reported previously (40). Therefore, this method employed an optimized chromatographic separation to avoid all the possible crosstalk mentioned before, resulting in high sensitivity and acceptable quantitative accuracy. Several laboratories reported a nice resolution for oxylipins (23, 41), which seems better than this method. However, it should be noted that this method contains more structurally similar oxylipins than theirs. For example, 16-HDHA was included in this method but absent in both methods, which had severe crosstalk with 17-HDHA ([supplemental Table S3](#)). We noted that the current chromatographic condition provided acceptable resolution for epoxy fatty acids, which might result in insufficient resolution of cis- and trans-epoxy fatty acids and lead to potential detection crosstalk and positive bias in sample analysis (42, 43).

In addition, this method is very practical and problem-solving because it is a powerful tool to provide answers to several common questions raised in the field. For example, some previous methods only covered the metabolites of ARA (44, 45) or ARA/LA (36, 46), which

may disregard the possible substrate competition among these PUFAs. In contrast, this method well quantifies the metabolites of ARA, LA, α -linolenic acid, and EPA simultaneously, which opens the possibility to collect evidence of possible substrate competition and other communications. Furthermore, unlike the existing method focusing on the metabolites of a specific metabolic branch (46) or some commercially available kits focusing on the individual metabolites like PGE₂ or LTB₄, this method simultaneously quantifies about 100 metabolites, covering most major metabolites mediated by COXs, LOXs, and CYPs, as well as some subsequent metabolic pathway like epoxide hydrolases and nonenzymatic reactions, which provides the possibility to quantitatively monitor the possible interactions among different metabolic pathways. For example, we found, in addition to acting on the target pathway, inhibition of soluble epoxide hydrolase also had an inhibitive impact on COX and LOX pathways but not following the metabolic shunting rule (47, 48). In addition, NSAIDs have been widely used for selective and nonselective inhibition of COX-1 or COX-2. Increased risks in cardiovascular events are a class side effect of nonaspirin NSAIDs (49). The dominant mechanism underlying NSAIDs-mediated cardiovascular is the imbalance between prothrombotic TXA₂ and antithrombotic prostacyclin I₂ (50, 51). Due to the instability of TXA₂ and prostacyclin I₂, their respective relatively stable metabolites TXB₂ and 6-keto-PGF_{1 α} are usually measured instead. Another theory is that inhibition of COX increases the vasoconstrictive and prothrombotic 20-HETE because COXs can mediate the metabolism of 20-HETE to form less active 20-OH-PGE₂, 20-OH-PGF_{2 α} , and others (52). However, up till now, there have not been solid clinic data to support these mechanisms mainly because these mediators are difficult to qualify. This newly established method not only has sufficient sensitivity to make it feasible to monitor 20-HETE, TXB₂, and 6-keto-PGF_{1 α} but also includes some quantifiable metabolites of them, including 20-OH-PGE₂, 20-OH-PGF_{2 α} , 11-dehydro TXB₂, 2,3-dinor-6-keto-PGF_{1 α} , etc., opening the possibility to test the above-mentioned theories translationally and clinically.

Overall, the newly established method made significant improvements in sample consumption, quantification capacity for low abundance oxylipins, and linear range with existing methods. It is believed that this method will greatly facilitate and advance the physiological, pathological, and pathophysiological function research of oxylipins.

Data Availability

All data are presented within the article and supplemental data. 

Supplemental Data

This article contains [supplemental data](#).

Acknowledgments

This work was cosupported by the Chongqing Postdoctoral Sustentation Fund (cstc2021jcyj-bshX0164), National Natural Science Foundation of China (82273408), and Chongqing Education Committee University Innovation Research Group Grant (CXQT21016).

Author Contributions

X. F. and J.-Y. L. conceptualization; X. F., H.-H. Y., and M.-J. W. methodology; X. F. writing—original draft; X. F. and J.-Y. L. funding acquisition; X. H., Q. J., and L.-T. Z. sample collection; J.-Y. L. supervision; J.-Y. L. writing—review and editing.

Author ORCIDi

Jun-Yan Liu  <https://orcid.org/0000-0002-3018-0335>

Conflicts of Interest

The authors declare that they have no conflicts of interest with the contents of this article.

Abbreviations

ACN, acetonitrile; ARA, arachidonic acid; COX, cyclooxygenase; CUDA, 12-(3-cyclohexan-1-yl-ureido) dodecanoic acid; CYP, cytochrome P450; DiHDPAs, dihydroxydocosapentaenoic acids; EpDPAs, epoxydocosapentaenoic acids; EpETEs, epoxyeicosatetraenoic acids; EpETrEs, epoxyeicosatrienoic acids; EpOMEs, epoxygenase-mediated epoxyoctadecenoic acids; HDHAs, hydroxydocosahexaenoic acids; HEPEs, hydroxyeicosapentaenoic acids; HQC, high quality control; LA, linoleic acid; LLOQ, lower limit of quantitation; LOD, limit of detection; LOX, lipoxygenase; LQC, low quality control; MQC, middle quality control; MRM, multiple reaction monitoring; NSAIDs, nonsteroidal anti-inflammatory drugs; PG, prostaglandin; Rt, retention time; S/N, signal-to-noise ratio; SPE, solid phase extraction; TX, thromboxane.

Manuscript received September 18, 2022, and in revised form October 6, 2022. Published, JLR Papers in Press, October 17, 2022, <https://doi.org/10.1016/j.jlr.2022.100302>

REFERENCES

- Gabbs, M., Leng, S., Devassy, J. G., Monirujjaman, M., and Aukema, H. M. (2015) Advances in our understanding of oxylipins derived from dietary PUFAs. *Adv. Nutr.* **6**, 513–540
- Zarate, R., el Jaber-Vazdekis, N., Tejera, N., Perez, J. A., and Rodriguez, C. (2017) Significance of long chain polyunsaturated fatty acids in human health. *Clin. Transl. Med.* **6**, 1–19
- Schunck, W. H., Konkel, A., Fischer, R., and Weylandt, K. H. (2018) Therapeutic potential of omega-3 fatty acid-derived epoxyeicosanoids in cardiovascular and inflammatory diseases. *Pharmacol. Ther.* **183**, 177–204
- Funk, C. D. (2001) Prostaglandins and leukotrienes: advances in eicosanoid biology. *Science*. **294**, 1871–1875
- Wang, B., Wu, L. J., Chen, J., Dong, L. L., Chen, C., Wen, Z., et al. (2021) Metabolism pathways of arachidonic acids: mechanisms and potential therapeutic targets. *Signal. Transduct. Target Ther.* **6**, 1–30
- Wang, C. J., Liu, W. L., Yao, L., Zhang, X. J., Zhang, X., Ye, C. J., et al. (2017) Hydroxyeicosapentaenoic acids and epoxyeicosatetraenoic acids attenuate early occurrence of nonalcoholic fatty liver disease. *Br. J. Pharmacol.* **174**, 2358–2372
- Leiria, L. O., Wang, C. H., Lynes, M. D., Yang, K. Y., Shamsi, F., Sato, M., et al. (2019) 12-lipoxygenase regulates cold adaptation and glucose metabolism by producing the omega-3 lipid 12-HEPE from brown fat. *Cell Metab.* **30**, 768–783
- Sapieha, P., Stahl, A., Chen, J., Seaward, M. R., Willett, K. L., Krah, N. M., et al. (2011) 5-lipoxygenase metabolite 4-HDHA is a mediator of the antiangiogenic effect of omega-3 polyunsaturated fatty acids. *Sci. Transl. Med.* **3**, 69ral2
- Napylov, A., Reyes-Garces, N., Gomez-Rios, G., Olkowitz, M., Lendor, S., Monnin, C., et al. (2020) In vivo solid-phase microextraction for sampling of oxylipins in brain of awake, moving rats. *Angew. Chem. Int. Edit.* **59**, 2392–2398
- Yu, Z. G., Xu, F. Y., Huse, L. M., Morisseau, C., Draper, A. J., Newman, J. W., et al. (2000) Soluble epoxide hydrolase regulates hydrolysis of vasoactive epoxyeicosatrienoic acids. *Circ. Res.* **87**, 992–998
- Deng, B. Q., Luo, Y., Kang, X., Li, C. B., Morisseau, C., Yang, J., et al. (2017) Epoxide metabolites of arachidonate and docosahexaenoate function conversely in acute kidney injury involved in gsk3 beta signaling. *Proc. Natl. Acad. Sci. U. S. A.* **114**, 12608–12613
- Jiang, J. G., Chen, C. L., Card, J. W., Yang, S. L., Chen, J. X., Fu, X. N., et al. (2005) Cytochrome p450 2j2 promotes the neoplastic phenotype of carcinoma cells and is up-regulated in human tumors. *Cancer Res.* **65**, 4707–4715
- Hall, C. N., Reynell, C., Gesslein, B., Hamilton, N. B., Mishra, A., Sutherland, B. A., et al. (2014) Capillary pericytes regulate cerebral blood flow in health and disease. *Nature* **508**, 55–60
- Misheva, M., Kotzamanis, K., Davies, L. C., Tyrrell, V. J., Rodrigues, P. R. S., Benavides, G. A., et al. (2022) Oxylipin metabolism is controlled by mitochondrial beta-oxidation during bacterial inflammation. *Nat. Commun.* **13**, 1–20
- Kong, C., Yan, X. B., Zhu, Y. F., Zhu, H. Y., Luo, Y., Liu, P. P., et al. (2021) Fusobacterium nucleatum promotes the development of colorectal cancer by activating a cytochrome p450/epoxyoctadecenoic acid axis via thr4/keap1/nrf2 signaling. *Cancer Res.* **81**, 4485–4498
- Stanford, K. I., Lynes, M. D., Takahashi, H., Baer, L. A., Arts, P. J., May, F. J., et al. (2018) 12,13-DiHOME: an exercise-induced lipokine that increases skeletal muscle fatty acid uptake. *Cell Metab.* **27**, 1111–1120
- Lynes, M. D., Leiria, L. O., Lundh, M., Bartelt, A., Shamsi, F., Huang, T. L., et al. (2017) The cold-induced lipokine 12,13-DiHOME promotes fatty acid transport into brown adipose tissue. *Nat. Med.* **23**, 631–637
- Nagatake, T., Shioyama, Y., Inoue, A., Kikuta, J., Honda, T., Tiwari, P., et al. (2018) The 17,18-epoxyeicosatetraenoic acid-g protein-coupled receptor 40 axis ameliorates contact hypersensitivity by inhibiting neutrophil mobility in mice and cynomolgus macaques. *J. Allergy Clin. Immunol.* **142**, 470–484
- Zhang, G. D., Panigrahy, D., Mahakian, L. M., Yang, J., Liu, J. Y., Lee, K. S. S., et al. (2013) Epoxy metabolites of docosahexaenoic acid (DHA) inhibit angiogenesis, tumor growth, and metastasis. *Proc. Natl. Acad. Sci. U. S. A.* **110**, 6530–6535
- Chhonker, Y. S., Bala, V., and Murry, D. J. (2018) Quantification of eicosanoids and their metabolites in biological matrices: a review. *Bioanalysis*. **10**, 2027–2046
- Wang, T., Li, H. N., Han, Y. Q., Wang, Y. W., Gong, J. C., Gao, K., et al. (2020) A rapid and high-throughput approach to quantify non-esterified oxylipins for epidemiological studies using online SPE-LC-MS/MS. *Anal. Bioanal. Chem.* **412**, 7989–8001
- Pedersen, T. L., Gray, I. J., and Newman, J. W. (2021) Plasma and serum oxylipin, endocannabinoid, bile acid, steroid, fatty acid and nonsteroidal anti-inflammatory drug quantification in a 96-well plate format. *Anal. Chim. Acta.* **1143**, 189–200
- Ostermann, A. I., Willenberg, I., and Schebb, N. H. (2015) Comparison of sample preparation methods for the quantitative analysis of eicosanoids and other oxylipins in plasma by means of LC-MS/MS. *Anal. Bioanal. Chem.* **407**, 1403–1414
- Kutzner, L., Rund, K. M., Ostermann, A. I., Hartung, N. M., Galano, J. M., Balas, L., et al. (2019) Development of an optimized LC-MS method for the detection of specialized pro-resolving mediators in biological samples. *Front. Pharmacol.* **10**, 169
- Luo, Y., Wang, L., Peng, A., and Liu, J. Y. (2019) Metabolic profiling of human plasma reveals the activation of 5-lipoxygenase in the acute attack of gouty arthritis. *Rheumatology*. **58**, 345–351

26. Colas, R. A., Gomez, E. A., and Dalli, J. (2020) Methodologies and procedures employed in the identification and quantitation of lipid mediators via LC-MS/MS
27. Schebb, N. H., Kuehn, H., Kahnt, A. S., Rund, K. M., O'Donnell, V. B., Flamand, N., *et al.* (2022) Formation, signaling and occurrence of specialized pro-resolving lipid mediators-what is the evidence so far? *Front. Pharmacol.* **13**, 475
28. Liakh, I., Pakiet, A., Sledzinski, T., and Mika, A. (2020) Methods of the analysis of oxylipins in biological samples. *Molecules.* **25**, 349
29. Gladine, C., Ostermann, A. I., Newman, J. W., and Schebb, N. H. (2019) MS-based targeted metabolomics of eicosanoids and other oxylipins: analytical and inter-individual variabilities. *Free Radic. Biol. Med.* **144**, 72–89
30. Sinha, G. (2022) Biomedicine doubt cast on inflammation's stop signals. *Science.* **376**, 565–566
31. Dasilva, G., Munoz, S., Lois, S., and Medina, I. (2019) Non-targeted LC-MS/MS assay for screening over 100 lipid mediators from ARA, EPA, and DHA in biological samples based on mass spectral fragmentations. *Molecules.* **24**, 2276
32. Kortz, L., Dorow, J., Becker, S., Thiery, J., and Ceglarek, U. (2013) Fast liquid chromatography-quadrupole linear ion trap-mass spectrometry analysis of polyunsaturated fatty acids and eicosanoids in human plasma. *J. Chromatogr. B.* **927**, 209–213
33. U.S. Food and Drug Administration. (2018) Bioanalytical Method Validation. Guidance for industry
34. *European Medicines Agency, Guideline on Bioanalytical Method Validation* (2011)
35. Gu, H. D., Liu, G. W., Wang, J., Aubry, A. F., and Arnold, M. E. (2014) Selecting the correct weighting factors for linear and quadratic calibration curves with least-squares regression algorithm in bioanalytical LC-MS/MS assays and impacts of using incorrect weighting factors on curve stability, data quality, and assay performance. *Anal. Chem.* **86**, 8959–8966
36. Yang, J., Schmelzer, K., Georgi, K., and Hammock, B. D. (2009) Quantitative profiling method for oxylipin metabolome by liquid chromatography electrospray ionization tandem mass spectrometry. *Anal. Chem.* **81**, 8085–8093
37. ICH Harmonized Tripartite Guidance: Validation of analytical procedures: Text and methodology Q2 (R1). London, (2005)
38. Gouveia-Figueira, S., Spath, J., Zivkovic, A. M., and Nording, M. L. (2015) Profiling the oxylipin and endocannabinoid metabolome by UPLC-ESI-MS/MS in human plasma to monitor postprandial inflammation. *PLoS One.* **10**, 1–29
39. Hartling, I., Cremonesi, A., Osuna, E., Lou, P. H., Lucchinetti, E., Zaugg, M., *et al.* (2021) Quantitative profiling of inflammatory and proresolving lipid mediators in human adolescents and mouse plasma using UPLC-MS/MS. *Clin. Chem. Lab. Med.* **59**, 1811–1823
40. Wang, Y., Armando, A. M., Quehenberger, O., Yan, C., and Dennis, E. A. (2014) Comprehensive ultra-performance liquid chromatographic separation and mass spectrometric analysis of eicosanoid metabolites in human samples. *J. Chromatogr. A.* **1359**, 60–69
41. Strassburg, K., Huijbrechts, A. M. L., Kortekaas, K. A., Lindeman, J. H., Pedersen, T. L., Dane, A., *et al.* (2012) Quantitative profiling of oxylipins through comprehensive LC-MS/MS analysis: application in cardiac surgery. *Anal. Bioanal. Chem.* **404**, 1413–1426
42. Rund, K. M., Heylmann, D., Seiwert, N., Wecklein, S., Oger, C., Galano, J.-M., *et al.* (2019) Formation of trans-epoxy fatty acids correlates with formation of isoprostanes and could serve as biomarker of oxidative stress. *Prostag. Oth. Lipid M.* **144**, 106334
43. Jiang, H. L., Quilley, J., Reddy, L. M., Falck, J. R., Wong, P. Y. K., and McGiff, J. C. (2005) Red blood cells: reservoirs of cis- and trans-epoxyeicosatrienoic acids. *Prostag. Oth. Lipid M.* **75**, 65–78
44. Wang, N. N., Dai, R. H., Wang, W. H., Peng, Y., Zhao, X. N., and Bi, K. S. (2016) Simultaneous profiling of eicosanoid metabolome in plasma by UPLC-MS/MS method: application to identify potential makers for rheumatoid arthritis. *Talanta.* **161**, 157–164
45. Shinde, D. D., Kim, K. B., Oh, K. S., Abdalla, N., Liu, K. H., Bae, S. K., *et al.* (2012) LC-MS/MS for the simultaneous analysis of arachidonic acid and 32 related metabolites in human plasma: basal plasma concentrations and aspirin-induced changes of eicosanoids. *J. Chromatogr. B.* **911**, 113–121
46. Newman, J. W., Watanabe, T., and Hammock, B. D. (2002) The simultaneous quantification of cytochrome p450 dependent linoleate and arachidonate metabolites in urine by HPLC-MS/MS. *J. Lipid Res.* **43**, 1563–1578
47. Liu, J. Y., Yang, J., Inceoglu, B., Qiu, H., Ulu, A., Hwang, S. H., *et al.* (2010) Inhibition of soluble epoxide hydrolase enhances the anti-inflammatory effects of aspirin and 5-lipoxygenase activation protein inhibitor in a murine model. *Biochem. Pharmacol.* **79**, 880–887
48. Schmelzer, K. R., Inceoglu, B., Kubala, L., Kim, I. H., Jinks, S. L., Eiserich, J. P., *et al.* (2006) Enhancement of antinociception by coadministration of nonsteroidal anti-inflammatory drugs and soluble epoxide hydrolase inhibitors. *Proc. Natl. Acad. Sci. U. S. A.* **103**, 13646–13651
49. Salvo, F., Antoniazzi, S., Duong, M., Molimard, M., Bazin, F., Fourier-Reglat, A., *et al.* (2014) Cardiovascular events associated with the long-term use of NSAIDs: a review of randomized controlled trials and observational studies. *Expert Opin. Drug Saf.* **13**, 573–585
50. Cheng, Y., Austin, S. C., Rocca, B., Koller, B. H., Coffman, T. M., Grosser, T., *et al.* (2002) Role of prostacyclin in the cardiovascular response to thromboxane A(2). *Science.* **296**, 539–541
51. FitzGerald, G. A. (2004) Coxibs and cardiovascular disease. *New Engl. J. Med.* **351**, 1709–1711
52. Liu, J. Y., Li, N., Yang, J., Li, N., Qiu, H., Ai, D., *et al.* (2010) Metabolic profiling of murine plasma reveals an unexpected biomarker in rofecoxib-mediated cardiovascular events. *Proc. Natl. Acad. Sci. U. S. A.* **107**, 17017–17022